Midinfrared optical excitations in undoped lamellar copper oxides

J. D. Perkins*
Department of Physics, Massachusetts Institute of Technology, Cambridge, Massachusetts 02139 and Center for Basic Sciences, National Renewable Energy Laboratory, Golden, Colorado 80401

R. J. Birgeneau
Department of Physics, Massachusetts Institute of Technology, Cambridge, Massachusetts 02139

J. M. Graybeal†
Department of Physics, Massachusetts Institute of Technology, Cambridge, Massachusetts 02139 and Department of Physics, University of Florida, Gainesville, Florida 32611

M. A. Kastner and D. S. Kleinberg
Department of Physics, Massachusetts Institute of Technology, Cambridge, Massachusetts 02139
(Received 2 April 1997; revised manuscript received 31 March 1998)

The weakly electric-dipole-allowed midinfrared excitations are studied in insulating single crystals of La_2CuO_4, $Sr_2CuO_2Cl_2$, and Nd_2CuO_4. These intrinsic excitations of the undoped CuO_2 layers are lower in energy than the charge-transfer excitation. Temperature-dependent optical-absorption measurements are presented from 10 to 450 K. Photoinduced absorption measurements on single-crystal La_2CuO_4 are also presented. Recent theoretical work and optical-absorption experiments on La_2NiO_4, as well as the copper oxides, provide strong evidence that a sharp absorption peak seen in all the copper oxides at photon energy ~0.4 eV and a related peak near 0.25 eV in La_2NiO_4 arise from phonon-assisted creation of a quasibound two-magnon state. A comparison between the intrinsic absorption in La_2NiO_4 and that in the copper oxides suggests that the broad midinfrared absorption bands observed between 0.4 and 1.2 eV in the undoped copper oxides have a different electronic origin. We discuss our measurements in regards to two proposed origins (phonon-multimagnon and exciton sidebands) for these broad higher-energy bands. We find that multimagnon and phonon sidebands associated with a Cu $d_{x^2-y^2} \rightarrow d_{3z^2-r^2}$ crystal-field exciton at ~0.5 eV plausibly explain the structure, strength, and polarization dependence of these broadbands. Direct observation of this exciton would unambiguously confirm or refute this model. [S0163-1829(98)01733-0]

I. INTRODUCTION

The lamellar copper-oxide superconductors are unusual in that they are derived from antiferromagnetic insulating host materials, such as La_2CuO_4, by chemical doping. An interesting feature common to the superconductors and the lightly doped materials is strong optical absorption in the midinfrared.[1–3] Recent experiments on the undoped insulators have revealed a variety of optical excitations in the same spectral range.[4–7] Understanding these electronic excitations of the undoped CuO_2 layers is not only intrinsically interesting, but also may provide insights into the origin of the doping-induced infrared absorption and perhaps the superconductivity itself.

It is now generally accepted that the undoped host materials are charge-transfer (CT) insulators with one $3d_{x^2-y^2}$ hole per copper site and a CT gap of ~2 eV. Reflectivity experiments show that, upon doping, oscillator strength is transferred from above to below the CT gap.[1] In heavily doped samples, strong, broad absorption extends from the CT gap to well below 0.1 eV.[1] Experiments on lightly oxygen-doped crystals show two non-free-carrier absorption bands below the CT gap.[8] The lower-energy band, centered at ~0.1 eV, is strongly temperature dependent[9] while the higher-energy band, peaked at ~0.5 eV, is nearly temperature independent. The lower-energy band arises from the photoionization of polarons bound to impurities.[9] However, for the ~0.5-eV band, the absence of sharp spectral features or dramatic temperature dependence has made a definitive interpretation difficult. Additional doping-induced absorption is also seen at ~1.5 eV.[8] It is now known[4] that there are intrinsic optical excitations near 0.5 and 1.5 eV in the undoped single-crystal oxides as well.[5–7]

Perkins *et al.*[4] reported measurements at 10 K for four undoped oxides: La_2CuO_4, Nd_2CuO_4, Pr_2CuO_4, and $Sr_2CuO_2Cl_2$. For the bands near 0.5 eV, the absorption coefficient is weak, roughly 10^3 times smaller than that in heavily doped samples. In all four compounds, the spectra display a sharp low-energy peak centered near 0.4 eV with a set of broader bands extending up to ~1 eV. The absorption features appear only for the electric-field polarized parallel to the CuO_2 layers with little sample-to-sample variation in the oscillator strength. Collectively, this demonstrates that the excitations are weakly electric-dipole-allowed intrinsic excitations of the undoped CuO_2 plane. Similar excitations have since been observed in $YBa_2Cu_3O_6$ by Grüninger *et al.*[10]

Perkins *et al.*[4] proposed that the sharp peak arises from the excitation of a Cu $d_{x^2-y^2}$ hole to the $d_{3z^2-r^2}$ state, that is, a Cu d-d^* crystal-field exciton. On the other hand, Lorenzana and Sawatzky[11,12] subsequently argued that the sharp

peak corresponds to phonon-assisted creation of a quasi-bound two-magnon state (labeled a ''bimagnon''). Recent optical absorption experiments by Perkins *et al.*[13] on La_2NiO_4, a spin $S=1$ isomorph of $S=\frac{1}{2}$ La_2CuO_4, reveal a weakly allowed electric-dipole band at $\sim$0.25 eV. The shape of this band in La_2NiO_4 and that of the sharp feature at $\sim$0.4 eV in La_2CuO_4 are well described by the theory of Lorenzana and Sawatzky for one-phonon–two-magnon absorption, thereby providing strong evidence that the 0.4-eV peak in the Cu oxides is a phonon-assisted bimagnon excitation. However, the broad higher-energy bands clearly seen in La_2CuO_4 are not observed in La_2NiO_4. This is inconsistent with an assignment of these bands to phonon-assisted magnetic excitations arising from the simplest Heisenberg antiferromagnet, one including only nearest-neighbor two-body interactions ($H=J\Sigma_{\langle N,N\rangle}\mathbf{S}_i\cdot\mathbf{S}_j$). Additional magnetic interactions, alternate electronic excitations, or other unexpected interactions must be present. Below, we discuss the Lorenzana and Sawatzky multimagnon scenario as well as the Perkins *et al.* model in which the broadbands result from magnons and phonons coupled to excitons. Specifically, sidebands associated with a Cu $d_{x^2-y^2}\rightarrow d_{3z^2-r^2}$ crystal-field exciton at $\sim$0.4–0.5 eV plausibly explain the strength, structure, and polarization dependence of the broad higher-energy bands. However, the low, $\sim$0.5 eV, exciton energy required is significantly lower than that predicted by cluster calculations[14–18] and the exciton itself has not been observed directly.

In this paper, we present spectra for La_2CuO_4, $Sr_2CuO_2Cl_2$, and Nd_2CuO_4 at temperatures ranging from 10 to 444 K. In addition, we compare the measured intrinsic absorption with both new photoinduced optical absorption data for an undoped La_2CuO_4 single crystal and existing data for oxygen-doped La_2CuO_{4+y}.[8]

Our paper is organized as follows: In Sec. II we provide details of the sample preparation and experimental measurements. In Sec. III we present the new experimental results. Section IV provides a discussion and finally, in Sec. V we summarize our conclusions.

II. EXPERIMENTAL PROCEDURES

Figure 1 shows the crystal structure of La_2CuO_4; in tetragonal $Sr_2CuO_2Cl_2$, the La is replaced by Sr and the apical O by Cl. At high temperature, both La_2CuO_4 and $Sr_2CuO_2Cl_2$ are tetragonal, but while $Sr_2CuO_2Cl_2$ remains tetragonal to 10 K or lower, La_2CuO_4 acquires a slight orthorhombic distortion below $\sim$530 K. In La_2CuO_4, the apical oxygen ions create a distorted octahedral coordination of the Cu ions, and in $Sr_2CuO_2Cl_2$, the apical Cl ions do the same. In contrast, Nd_2CuO_4 and Pr_2CuO_4 are tetragonal with square-planar-coordinated Cu sites and no apical ions. With the differing chemical compositions and out-of-plane structures, the only structural component common to these four materials is the two-dimensional (2D), approximately square-planar, CuO_2 layer characteristic of all of the copper-oxide high-temperature superconductors. The structure of La_2NiO_4 is the same as that of La_2CuO_4 but with Ni in place of Cu.

All four copper oxides are spin-$\frac{1}{2}$ Heisenberg antiferromagnets with comparable nearest-neighbor Cu-Cu exchange

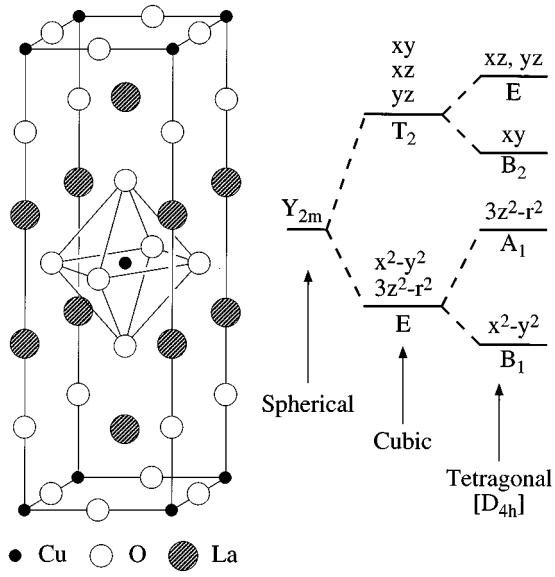

FIG. 1. Left: The crystal structure for tetragonal La_2CuO_4 (T phase). In isomorphic $Sr_2CuO_2Cl_2$, the La is replaced with Sr and the apical O with Cl. Right: Schematic splitting of Cu $3d$-state hole energies in an elongated tetragonal symmetry.

interactions J as measured by Raman scattering (see, for example, Refs. 19–22). For La_2CuO_4, $J\sim0.13$ eV. La_2NiO_4, on the other hand, is a spin-1 Heisenberg antiferromagnet with $J\sim0.03$ eV.[22,23] $Sr_2CuO_2Cl_2$ is the best experimental realization of the 2D spin $S=\frac{1}{2}$ square-lattice Heisenberg antiferromagnet studied to date.[24]

The Nd_2CuO_4 and most of the La_2CuO_4 crystals were grown by the top-seeded solution method in Pt crucibles using CuO flux.[25,26] Additional La_2CuO_4 crystals were grown by the traveling solvent floating-zone technique[27] and are thus free of Pt. As grown, the La_2CuO_4 crystals contain excess oxygen resulting in a doping level of $\sim0.5\times10^{-2}$ holes/Cu ion.[28,29] To remove the excess holes, the La_2CuO_4 samples are annealed for 45 min at 900 °C in a vacuum of $P\leqslant4\times10^{-6}$ Torr.[30] To obtain sample thicknesses ranging from $\sim$30–200 μm, the annealed La_2CuO_4 and as-grown Nd_2CuO_4 samples are then polished using diamond grit on tin laps. Finally, just prior to measurement, the La_2CuO_4 and Nd_2CuO_4 crystals are etched in 1% Br in isopropanol to remove any surface damage or contamination.

The $Sr_2CuO_2Cl_2$ crystals are grown by slowly cooling a stoichiometric melt in a Pt crucible.[31,32] As-grown $Sr_2CuO_2Cl_2$ is stoichiometric and cannot be readily doped. It is micaceous, allowing optical quality surfaces to be easily cleaved from the as-grown crystals.

To allow transmission experiments, yet prevent stray light from passing around the crystal edges, the samples, typically 1–3 mm in width, are mounted on copper backing plates over an appropriate diameter hole. Optical transmission spectra in the photon-energy range 0.1 to 2 eV are obtained using a grating monochromator. The inset in Fig. 2 shows the three distinct polarizations possible for optical measurements of dipole excitations in uniaxial crystals. Measurements were made for La_2CuO_4, $Sr_2CuO_2Cl_2$, and Nd_2CuO_4 in the α polarization (electric field $\mathbf{E}\|CuO_2$ layer and wave vector $\mathbf{k}\perp$ layer). Additional La_2CuO_4 samples have been

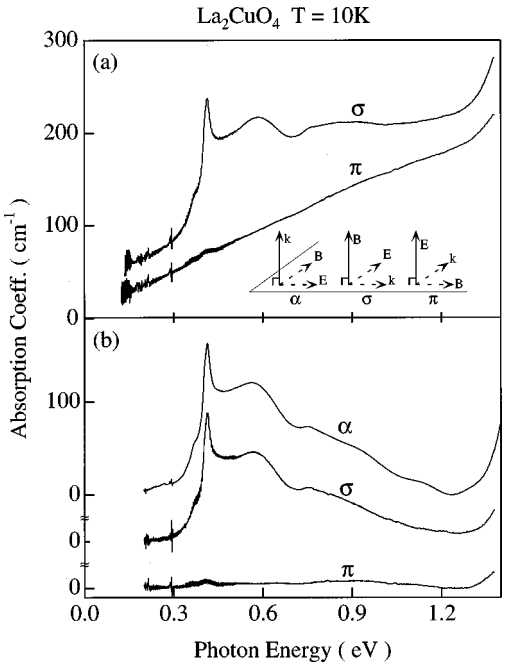

FIG. 2. (a): La_2CuO_4 absorption coefficient vs photon energy for σ and π polarizations at $T=10$ K for two crystals. Also in (a) is a sketch of the three distinct dipole polarizations for a uniaxial crystal. For α and σ polarization, the electric field lies in the CuO_2 plane. For the π polarization, the electric field is perpendicular to the CuO_2 plane. The dashed axes lie in the plane, the solid axes are perpendicular to the plane. Panel (b): La_2CuO_4 absorption coefficient vs photon energy for α, σ, and π polarizations after subtracting the background. Interference fringes are seen in some of these spectra.

polished with large faces perpendicular to the layers for measurements with **k** in the CuO_2 layer for both σ (**E**$\|$layer) and π (**E**$\perp$ layer) polarizations. The sample thickness, $\sim$10–200 μm, is determined from both direct mechanical measurement and observed interference fringes in the spectra.

For the photoinduced absorption experiments, the transmission was measured in σ polarization using a probe beam chopped at 400 Hz. The sample was optically pumped with an unfocused 7-mW cw HeNe laser operating at 632.8 nm. For the nominally π-polarized pump beam, any σ-polarized component is strongly absorbed, but the π-polarized component penetrates the sample. We assume that, because of imperfections, there is some depolarization of the π-polarized beam thereby creating electron-hole pairs throughout the sample. A mechanical shutter chops the pump beam at 5 Hz and a second lock-in amplifier measures the 5-Hz variation in the output of the first lock-in amplifier.

The optical spectra are presented in terms of the absorption coefficient α which, including multiple internal reflections, but ignoring interference effects, is related to the measured transmission T by $T=(1-R)^2e^{-\alpha d}/(1-R^2e^{-2\alpha d})$, where d is the sample thickness and R is the reflectivity. In the undoped lamellar copper oxides, the reflectivity is small and nearly constant throughout the infrared ($\sim$0.15 for La_2CuO_4, Ref. 30). Then, since for the sample thicknesses used $\alpha d>1$, we use $\alpha d\approx-\ln(T)$. In addition, aperturing of the probe beam by the sample mounting plate can produce a wavelength-independent offset as well. The background subtraction discussed in the next section removes any such offset.

III. EXPERIMENTAL RESULTS

A. Spectra at 10 K

Figure 2(a) shows the σ- and π-polarized absorption spectra measured at 10 K for La_2CuO_4. A comparison of the two spectra suggests that the σ-polarized absorption bands are superposed on a polarization-independent background that is nearly linear in photon energy. This background, which varies from sample to sample, does not scale with sample thickness and is reduced in magnitude with improved surface preparation. In particular, the smallest background is found for freshly cleaved $Sr_2CuO_2Cl_2$ samples. Hence, the background is believed to arise from surface scattering. Therefore, to display more clearly the bulk absorption of interest, an appropriate background is subtracted from all the measured spectra. For each σ-polarized La_2CuO_4 spectrum, the background is taken to be the π spectrum measured at the same temperature plus a constant. For the α spectra no alternate polarization spectra are possible. Therefore, as suggested by Fig. 2(a), a linear background is used.

Figure 2(b) shows α, σ, and π spectra for La_2CuO_4 measured at 10 K with the linear background subtracted. As noted previously,[4] the structure seen in the α-polarized spectrum appears in σ polarization but is absent in π polarization. La_2CuO_4 is the only material for which appropriate samples for σ- and π-polarized spectra could be prepared. The Nd_2CuO_4 and Pr_2CuO_4 crystals grow as thin plates with large c-axis faces, thus making σ- and π-polarized measurements impractical. Likewise, $Sr_2CuO_2Cl_2$ is too micaceous to prepare samples for σ- and π-polarized measurements. The small features seen in π polarization for La_2CuO_4 near the energy of the sharp peak are most likely α- and σ-polarized features appearing because of slight misalignment.

The selection rules governing dipole optical excitations in a uniaxial crystal are that bands appearing in α and σ but not in π or only in π are electric-dipole allowed, whereas bands that appear in π and α but not σ or only in σ are magnetic-dipole allowed. As seen in Fig. 2(b), the absorption features are seen in α and σ but not π polarization, that is, only when the electric field lies parallel to the CuO_2 plane. Hence, these are electric-dipole excitations.

To compare the strength of the absorption with that measured in other experiments, it is useful to calculate the oscillator strength. In units of electrons per Cu site, the oscillator strength is given by

$$f=\frac{2c\sqrt{\varepsilon_1}}{\pi}\left(\frac{m^*}{4\pi Ne^2}\right)\int\alpha(\omega)d\omega, \tag{1}$$

where N is the number of Cu sites per cm^3 and m^* is the electron effective mass. Using m^* equal to the bare electron mass, the oscillator strength for the entire absorption spectrum from $\sim$0.2 to 1.2 eV in La_2CuO_4 is $\sim10^{-4}$ electrons/Cu. By comparison, in lightly oxygen-doped La_2CuO_{4+y}, Thomas *et al.*[8] measure an oscillator strength of $\sim2\times10^{-2}$ electrons/Cu for the same spectral region. The small oscillator strength we measure raises the possibility that the observed absorption results from impuri-

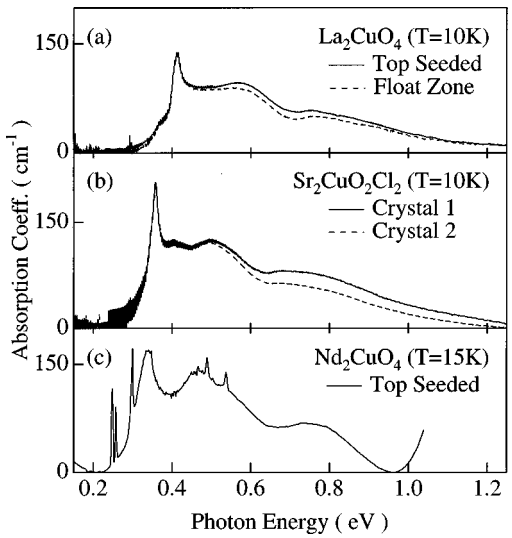

FIG. 3. Absorption coefficient vs photon energy at $T=10$ K for several crystals. Panel (a) compares top-seeded and float-zone-grown La_2CuO_4 crystals in the σ polarization. Panel (b) compares two $Sr_2CuO_2Cl_2$ crystals grown from different starting materials in the α polarization. The difference in the absorption in the $Sr_2CuO_2Cl_2$ crystals at ~0.8 eV probably arises from the background subtraction. Panel (c) shows the α-polarized spectra for one Nd_2CuO_4 crystal.

ties or defects. In Fig. 3 we show the absorption spectra for five different samples measured at 10 K. For the thinner samples, interference fringes are seen. Figure 3(a) compares La_2CuO_4 crystals grown by the top-seeded solution growth and floating-zone methods. The floating-zone crystals are free of Pt impurities known to exist in the top-seeded solution growth crystals. Figure 3(b) compares two crystals of $Sr_2CuO_2Cl_2$ grown from different starting materials. In the region of the sharp peak, the spectra are independent of growth technique or starting material. The minor differences at higher energies probably arise from background subtraction errors. Figure 3(c) shows the absorption spectrum of a Nd_2CuO_4 crystal. The additional sharp absorption lines not seen in La_2CuO_4 or $Sr_2CuO_2Cl_2$ are Nd^{+3} crystal-field excitations made weakly allowed by the lack of inversion symmetry at the Nd site.[33,34] Similar Pr^{+3} crystal-field excitations are seen in Pr_2CuO_4.[4] Examining all three panels in Fig. 3, one finds that the oscillator strength is quite similar, not only for different crystals of the same material, but also for different materials. As the impurity species and concentration, although low, clearly vary between the measured samples, the observed uniformity indicates that the excitations are indeed intrinsic. Quantitatively similar absorption spectra have also been observed by Grüninger *et al.*[10] in single crystals of the bilayer copper oxide $YBa_2Cu_3O_6$. Hence, on the basis of their universality and common strength we conclude that the measured spectra correspond to intrinsic, weakly electric-dipole-allowed, excitations of the undoped CuO_2 plane.

The spectra in Fig. 4 show that there are additional absorption bands at ~1.5–1.7 eV in both La_2CuO_4 and $Sr_2CuO_2Cl_2$. Note that the typical absorption coefficient for this band is $\sim 1000\ cm^{-1}$ or about ten times larger than that for the absorption near ~0.5 eV (an arrow highlights the

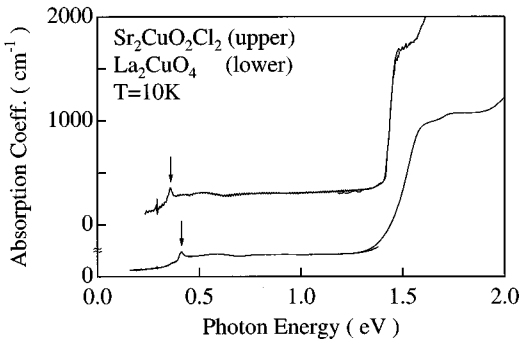

FIG. 4. Absorption coefficient vs photon energy in $Sr_2CuO_2Cl_2$ (upper trace) and La_2CuO_4 (lower trace) at $T=10$ K. The arrows indicate the ~0.4-eV absorption structure displayed more clearly in Fig. 3. An additional absorption band is seen at ~1.5 eV in both materials and another at 1.7 eV in La_2CuO_4. The charge-transfer absorption edge begins at 2.0 eV in La_2CuO_4 and at 1.65 eV in $Sr_2CuO_2Cl_2$.

sharp ~0.4-eV peak). Earlier reflectivity measurements on single-crystal La_2CuO_4 by Falck *et al.*[30] found an excitonic peak near 1.75 eV.

Several material-specific absorption features in Fig. 3 are worth noting. In La_2CuO_4, at low temperatures, a shoulder near 0.37 eV is evident on the low-energy side of the sharp peak. This shoulder appears with similar magnitude in every sample of La_2CuO_4 measured, and is therefore believed to be intrinsic. In the $Sr_2CuO_2Cl_2$ spectra shown in Fig. 3(b), a small feature can be seen at ~0.4 eV, just above the primary peak. This feature is more evident in data to be shown later (see Fig. 6). The strength of this feature varies significantly from sample to sample and day to day, and similar features are not seen in the other three materials studied. This lack of reproducibility and the presence of strong H_2O absorption bands in this photon-energy range suggest that these features are not intrinsic to $Sr_2CuO_2Cl_2$.

B. Temperature dependence

Absorption spectra have been measured from 10 to 300 K for La_2CuO_4, 10 to 444 K for $Sr_2CuO_2Cl_2$, and 10 to 300 K for Nd_2CuO_4. Figure 5 shows the σ-polarized absorption spectra for La_2CuO_4; an additional spectrum taken at 90 K is essentially identical to the 10-K spectrum. As is evident in the figure, the sharp peak at ~0.4 eV broadens and shifts to lower energy with increasing temperature. Above the sharp

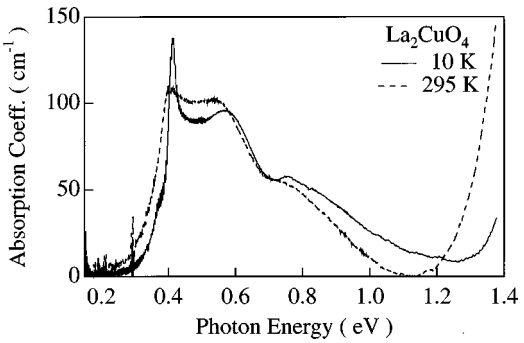

FIG. 5. La_2CuO_4 absorption coefficient vs photon energy in σ polarization at $T=10$ K and $T=295$ K.

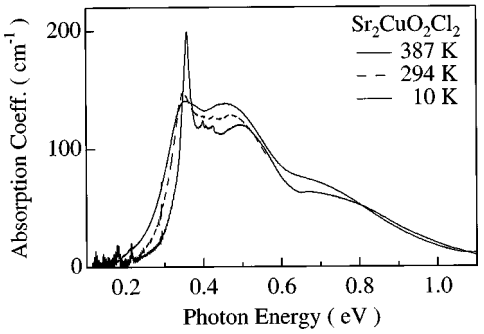

FIG. 6. $Sr_2CuO_2Cl_2$ absorption coefficient vs photon energy in α polarization at $T=10$, 294, and 387 K.

peak, the spectrum is weakly temperature dependent. In Fig. 6, we show α-polarized absorption spectra for $Sr_2CuO_2Cl_2$ at three representative temperatures. The overall temperature dependence is quite similar to that seen in La_2CuO_4. In particular, we note that no dramatic change in the absorption spectrum is seen above the Néel temperature which is ~256 K in $Sr_2CuO_2Cl_2$, as measured by neutron scattering.[24]

Figure 7 shows a series of σ spectra for La_2CuO_4 from 10 to 295 K in the vicinity of the sharp peak. Note the offsets used to display the data more clearly. For each spectrum, the featureless π-polarized spectrum measured at the same temperature provides the energy-dependent background apart from a constant offset. For the spectra taken at 10, 90, and 295 K, the offset is chosen such that at ~0.2 eV the absorption is zero. At the other temperatures, the spectra have not been measured for photon energies below ~0.33 eV, thereby necessitating an alternative normalization scheme. Figure 5 shows that the absorption coefficient is nearly the same at ~0.6 eV for $T=10$ and 295 K. Hence, for the other spectra, the offset is chosen to match the 10-K spectra at 0.56 eV, the highest photon energy examined at all temperatures. Figure 8

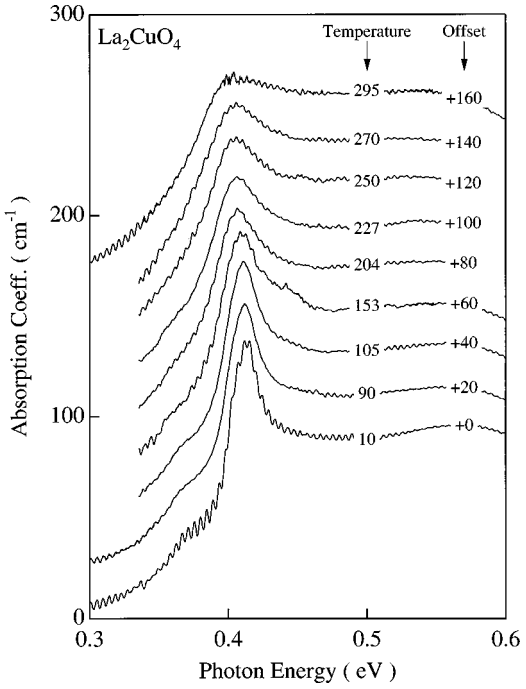

FIG. 7. La_2CuO_4 absorption coefficient vs photon energy in σ polarization at several temperatures. Note the indicated offsets.

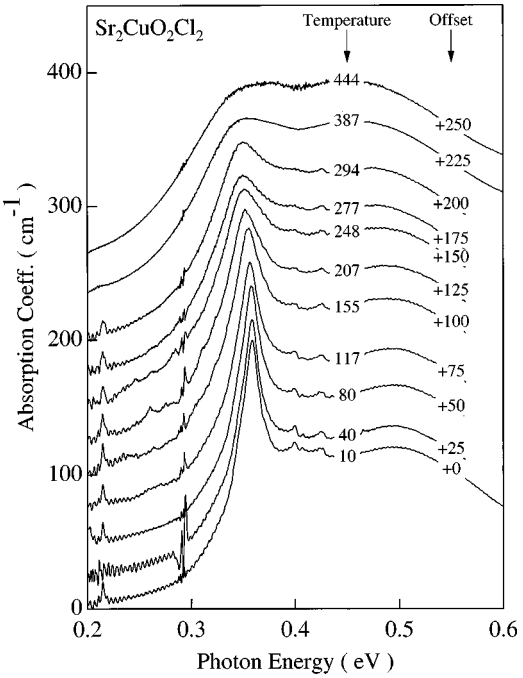

FIG. 8. $Sr_2CuO_2Cl_2$ absorption coefficient vs photon energy in α polarization at several temperatures. Note the indicated offsets. A different crystal was used for the 387- and 444-K spectra.

shows similar spectra for $Sr_2CuO_2Cl_2$ measured in α polarization. For each spectrum, a linear background has been subtracted with the slope chosen from the 10-K data and the offset chosen to set the absorption at ~0.15 eV to zero. In Fig. 9, we show α-polarized absorption spectra for Nd_2CuO_4 at 15, 105, 213, and 291 K.

We summarize, in Fig. 10, the temperature dependence of the sharp-peak energy, width, and oscillator strength for La_2CuO_4 and $Sr_2CuO_2Cl_2$. Between 10 and 300 K the peak energy decreases by ~0.01 eV in both La_2CuO_4 and $Sr_2CuO_2Cl_2$. Figure 10(b) shows twice the half width at half maximum measured on the low-energy side of the sharp peak. Measured in this way, the peak width is nearly identical in La_2CuO_4 and $Sr_2CuO_2Cl_2$. The sharp peak in La_2CuO_4 is broader on the high-energy side than that in $Sr_2CuO_2Cl_2$, but not on the low-energy side, when the shoulder is eliminated. The oscillator strength in Fig. 10(c) is twice the

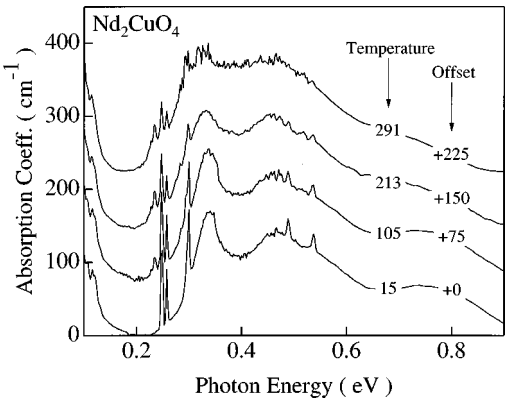

FIG. 9. Nd_2CuO_4 absorption coefficient vs photon energy in α polarization at several temperatures. Note the indicated offsets.

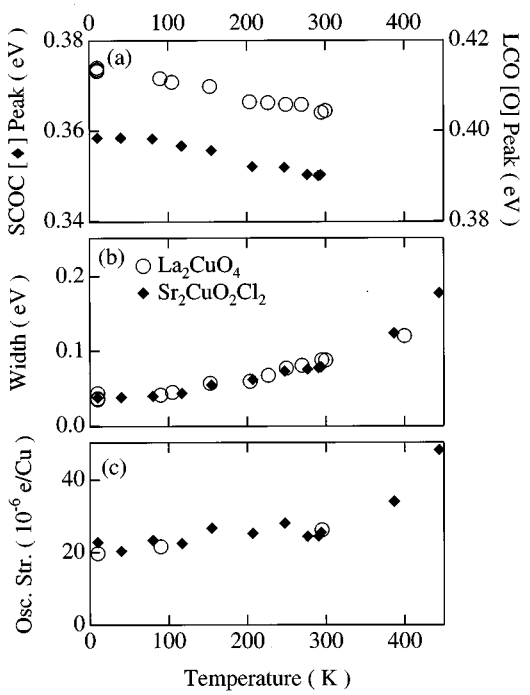

FIG. 10. Panel (a): Empirical peak position as a function of temperature for primary peak in $Sr_2CuO_2Cl_2$ (◆, left) and La_2CuO_4 (○, right). Panel (b): Empirical primary peak width as a function of temperature in $Sr_2CuO_2Cl_2$ (◆) and La_2CuO_4 (○). The reported width is twice the half width at half maximum measured from the peak to the low-energy side. Panel (c): Oscillator strength of primary peak as a function of temperature in $Sr_2CuO_2Cl_2$ (◆) and La_2CuO_4 (○). To avoid contributions of the higher-energy bands, the reported strength is twice the integrated strength from the low-energy side to the peak maximum.

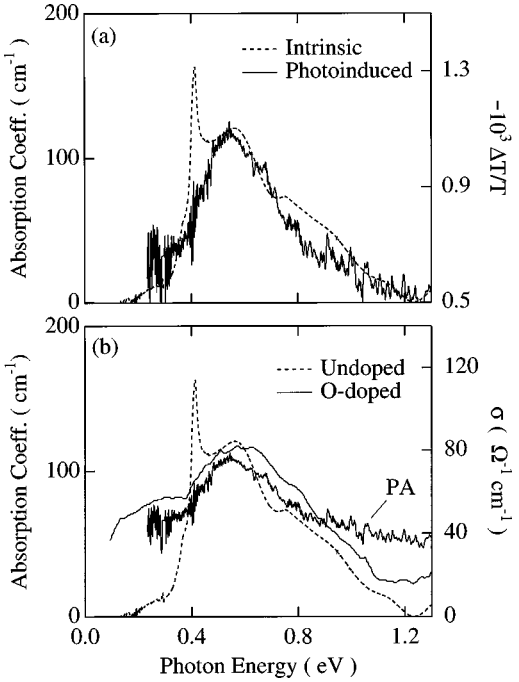

FIG. 11. Panel (a): Comparison of intrinsic absorption (left axis) in undoped La_2CuO_4 with photoinduced absorption (PA) (right axis) in the same crystal. Note that the PA axis minimum is not zero. Panel (b): Comparison of intrinsic absorption (left axis) in undoped La_2CuO_4 with the optical conductivity measured in lightly oxygen-doped La_2CuO_{4+y} (right axis) [Thomas *et al.* (Ref. 8)]. The PA from panel (a) is also shown with no zero offset. For the PA spectrum, the peak value at 0.54 eV is $-\Delta T/T = 1.1\times10^{-3}$.

strength integrated from the low-energy side up to the peak maximum. The low-energy limit of the integration is 0.16 eV in La_2CuO_4 and 0.145 eV in $Sr_2CuO_2Cl_2$. The growth of the oscillator strength with increasing temperature primarily reflects the increase of the peak width with temperature.

C. Photoinduced absorption

A natural question to ask is whether the absorption observed in the undoped materials has the same origin as that observed in the doped copper oxides. The comparisons shown in Fig. 11 suggest that, at least in lightly doped samples, the absorption processes might be of the same origin. Figure 11(a) compares the intrinsic absorption (left axis) with the photoinduced absorption (right axis) measured in the same La_2CuO_4 single crystal. For this comparison a constant background has been subtracted from the photoinduced spectrum. The pump beam with photon energy above the CT gap creates separated electrons and holes.[35] Thus, the photoinduced absorption spectrum corresponds to the modulation resulting from the addition of charge carriers. The photoinduced spectrum we measure for a La_2CuO_4 single crystal is qualitatively similar to that measured previously by Kim, Cheong, and Fisk[36] on a powdered sample. Figure 11(b) compares the intrinsic absorption in La_2CuO_4 (left axis) with that measured by Thomas *et al.*[8] in lightly oxygen-doped La_2CuO_{4+y} (right axis), as well as the photoinduced spectrum with no background subtracted.

Excepting the sharp 0.4-eV peak, for both chemical and photogenerated doping, the doping-induced band has similar energy and width to the intrinsic absorption in undoped samples. It is possible that the charge carriers introduced by doping may strengthen the electric-dipole character of intrinsic, but not fully dipole-allowed, excitations of the undoped copper oxides. For example, in electroreflectance measurements on La_2CuO_4, the electric-dipole forbidden Cu d-d^* excitons are made weakly allowed and hence observable by the perturbing electric field.[5] However, answering this question unambiguously requires a dedicated set of experiments to measure systematically the evolution of the absorption with doping in very lightly doped samples. Note also that the component of the doping-induced absorption near 0.2 eV, clearly observed in lightly oxygen doped La_2CuO_{4+y} [Fig. 11(b), solid line], is absent in the undoped La_2CuO_4 crystal [Fig. 11(b), dashed line]. Falck *et al.* have shown that this lower-energy absorption arises from the photoionization of impurity-trapped polarons.[9] Hence, its absence in our measured spectra supports our assertion that the observed absorption features correspond to intrinsic excitations of the undoped CuO_2 plane.

IV. DISCUSSION

A. Phonon-assisted two-magnon bound state

According to Lorenzana and Sawatzky, the sharp feature in the spectra of La_2CuO_4 and La_2NiO_4 results from phonon plus two-magnon excitations with magnon-pair momentum

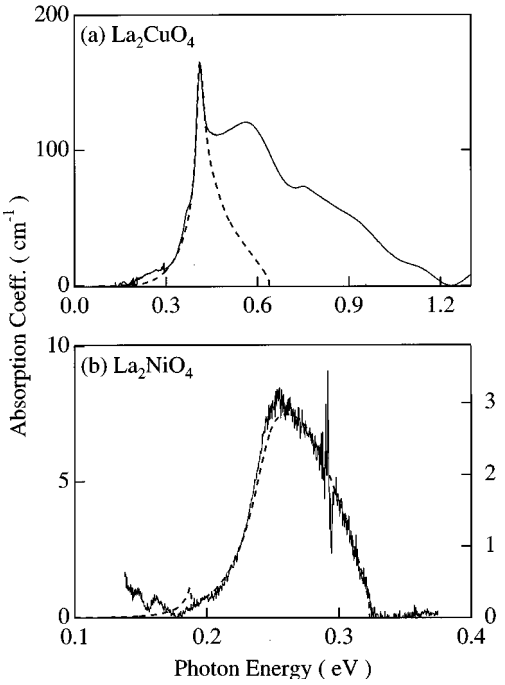

FIG. 12. Comparison of measured intrinsic electric-dipole absorption with theoretical prediction for phonon-assisted two-magnon absorption from Lorenzana and Sawatzky (Refs. 11 and 12). Experimental spectra measured at $T=10$ K. Panel (a): La_2CuO_4. The theory curve (dashed) is scaled by ~ 3 to match the experimental spectra (solid). Panel (b): La_2NiO_4. Left axis, measured absorption (solid line). Right axis, predicted theoretical absorption (dashed line).

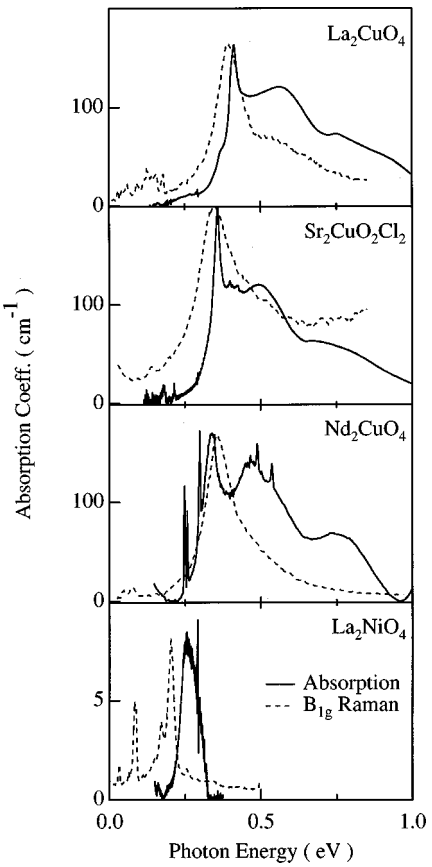

FIG. 13. Comparison of intrinsic electric-dipole absorption (solid line) and B_{1g} Raman spectra (dashed line). La_2CuO_4, Nd_2CuO_4, and La_2NiO_4: Raman measured at $T=30$ K [Sugai *et al.* (Ref. 22)]. $Sr_2CuO_2Cl_2$: Raman measured at $T=300$ K [Tokura *et al.* (Ref. 20)]. Absorption measured at $T\sim 10$ K in all.

near $(\pi,0)$.[37] Therefore, in plotting the theoretical spectra (Fig. 12), the phonon energy is taken to be 0.080 eV for La_2CuO_4 (Ref. 38) and 0.066 eV for La_2NiO_4,[39] which are the pertinent in-plane Cu-O and Ni-O stretching modes at $(\pi,0)$. For La_2NiO_4, we use $J=0.03$ eV, as found by Nakajima *et al.*[23] from neutron scattering and by Sugai *et al.*[22] from two-magnon Raman scattering. For La_2CuO_4, J is chosen so that the energy of the calculated peak coincides with that measured experimentally.[12] The value used, $J=0.121$ eV, is roughly 9% smaller than the 0.135 eV found by neutron and Raman scattering.[19,40–42]

Using the effective charge calculated by Lorenzana and Sawatzky, the calculated absorption strength is about three times smaller than that measured experimentally for both La_2CuO_4 and La_2NiO_4. In Figs. 12(a) and 12(b), the vertical axes are scaled so that the calculated absorption matches that measured experimentally at the sharp peak. It is clear that the agreement between theory and experiment is excellent for La_2NiO_4.

The measured and calculated spectra shown in Fig. 12 make apparent two important differences between the optical spectra of La_2CuO_4 and La_2NiO_4. First, the sharp peak, corresponding to one-phonon–two-magnon absorption, is markedly sharper relative to the peak energy in the copper oxides than in the nickel oxides. Second, while the broad higher-energy bands in La_2CuO_4 comprise the majority of the spectral weight, in La_2NiO_4 no such bands are observed.

As evident from Fig. 12, the theory obviously accounts for the difference in peak shape in the two materials. For both $S=\frac{1}{2}$ La_2CuO_4 and $S=1$ La_2NiO_4, Lorenzana and Sawatzky find a saddle point in the interacting two-magnon dispersion relation at magnon-pair momentum $(\pi,0)$ resulting in a Van Hove singularity in the two-magnon-pair density of states.[11] Furthermore, the strong magnon-magnon interaction at $(\pi,0)$ lowers the interacting magnon-pair energy enough so that there exists only a small density of free two-magnon states into which the interacting two-magnon state can decay. Accordingly, the excitation spectrum is relatively sharp. The one-phonon–two-magnon absorption spectrum for La_2CuO_4 is sharper than that for La_2NiO_4 because the stronger magnon-magnon interactions for $S=\frac{1}{2}$ than for $S=1$ enhance this effect.

It is interesting to compare the Raman and infrared absorption spectra as shown in Fig. 13. In La_2NiO_4 (bottom panel), the measured phonon-assisted two-magnon absorption (solid line) is broader and roughly one optical phonon energy higher than the two-magnon Raman peak (dashed line). This is in accord with the intuitive notion that adding a phonon to a two-magnon excitation will both broaden the resultant line shape and shift it to higher energy. Comparisons of the absorption and Raman spectra of the 3D $S=1$ antiferromagnets NiO (Ref. 43) and $KNiF_3$ (Refs. 44 and 45) yield qualitatively similar conclusions. In contrast, as shown in Fig. 13, for the $S=\frac{1}{2}$ copper oxides La_2CuO_4, $Sr_2CuO_2Cl_2$, and Nd_2CuO_4, the narrow peak corresponding

to phonon-assisted bimagnon absorption is both sharper than and nearly degenerate in energy with the two-magnon Raman peak. This is explained by the theory of Lorenzana and Sawatzky. The Raman-scattering peak results from two-magnon excitations with magnon-pair momentum $\mathbf{k}=0$, whereas the optical absorption, which requires the creation of a phonon, is dominated by two-magnon excitations at $\mathbf{k}=(\pi,0)$ where the magnon-magnon interaction is stronger than at $\mathbf{k}=0$. For the particular case of a spin-$\frac{1}{2}$ 2D square-lattice Heisenberg antiferromagnet with J of order 100 meV, the difference in the $\mathbf{k}=0$ and $\mathbf{k}=(\pi,0)$ magnon-magnon interaction is comparable to an optical phonon energy.[11,39,42] Hence, the near degeneracy of the absorption and Raman-scattering peaks in the undoped $S=\frac{1}{2}$ copper oxides apparently results from a coincidental near cancellation of the magnon-magnon interaction and the optical-phonon energy in the copper oxides.

At low temperatures, only phonon-creation excitations can occur. However, at elevated temperatures, the annihilation of thermally excited phonons should result in additional absorption. As the characteristic phonon energy is quite high (~70–80 meV), phonon-annihilation absorption will not dominate the absorption, even at 450 K. Furthermore, the broadening of the sharp peak with increasing temperature makes the identification of an annihilation peak difficult. Therefore, in the absence of an explicit theory for the temperature dependence of the line shape, we have made an iterative analysis to determine if the measured spectra are consistent with a superposition of creation and annihilation peaks. Assuming a phonon energy of $E_p=0.07$ eV,[11,39,46] as appropriate for phonon-assisted two-magnon absorption in $Sr_2CuO_2Cl_2$, the annihilation band strength would be much smaller than the creation band strength for the temperatures studied. Therefore, we take the measured spectrum as a first approximation to the creation band. From this, an annihilation band is derived by scaling the creation band by $e^{-E_p/kT}$ and shifting it down in photon energy by $2E_p$. The resulting annihilation-band spectrum is subtracted from the measured spectrum to yield a new creation band, and the process is iterated until there is no visible change in the derived bands. To define a consistent zero for the derived spectra, the creation-band absorption is taken to be zero at 0.15 eV. Figure 14 shows the iteratively derived bands in $Sr_2CuO_2Cl_2$ at 291, 387, and 444 K. We find that the low-energy broadening of the sharp peak is consistent with a phonon-assisted absorption process.

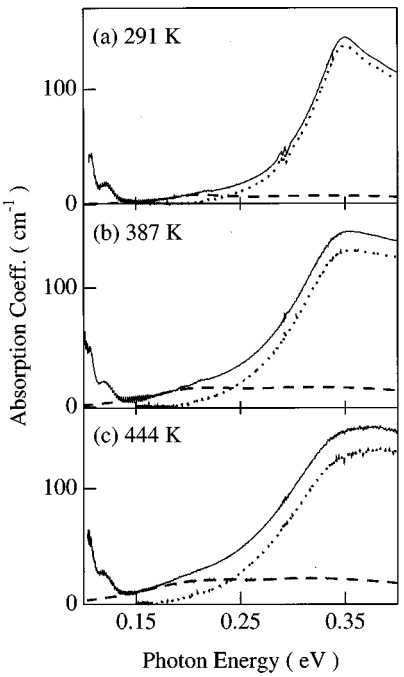

FIG. 14. Panels (a)–(c): Iteratively derived phonon-annihilation and creation bands in $Sr_2CuO_2Cl_2$ at various temperatures: (a) 291 K, (b) 387 K, and (c) 444 K. The solid line is the measured spectrum. The dashed and dotted lines are the derived annihilation and creation bands, respectively.

B. Broad 0.4–1-eV absorption

As evident in Fig. 13, in addition to the sharp ~0.4-eV peak, broad higher-energy absorption bands of comparable intensity extend from ~0.4 to 1 eV in the copper oxides, but no such bands are seen in La_2NiO_4.[13] Specifically, any absorption for La_2NiO_4 in the energy range 0.33 to 0.5 eV corresponds to less than one-tenth the oscillator strength in the phonon-assisted two-magnon band,[13] whereas for La_2CuO_4 the strength of the extended absorption is at least five times larger than that of the primary peak. Thus, the relative sideband strength decreases by at least a factor of 50 between $S=\frac{1}{2}$ La_2CuO_4 and $S=1$ La_2NiO_4. Lorenzana and Sawatzky suggest that phonon-assisted multimagnon[47] excitations involving more than two magnons may explain the broad higher-energy bands in La_2CuO_4.[11,12,48] However, in our view, the absence of analogous bands in La_2NiO_4, compared to their dominance in La_2CuO_4, is inconsistent with the multimagnon excitations of a *simple* Heisenberg antiferromagnet ($H_0=J\Sigma_{\langle NN\rangle}\mathbf{S}_i\cdot\mathbf{S}_j$).

To first order in the phonon coordinate $\mathbf{u}_{ph}$ and the optical electric field $\mathbf{E}$ a coupling between phonons and the Cu-Cu exchange constant J yields a Hamiltonian of the form

$$H=H_0+Q_{\text{eff}}\sum_{\langle NN\rangle}(\mathbf{u}_{ph}\cdot\mathbf{E})(\mathbf{S}_i\cdot\mathbf{S}_j), \tag{2}$$

where H_0 is the unperturbed spin Hamiltonian and the expansion coefficient Q_{eff}, the effective charge. The $\mathbf{u}_{ph}$ term generates phonons and the $\mathbf{S}_i\cdot\mathbf{S}_j$ term, magnon-pair and higher-order multimagnon excitations. For a Heisenberg antiferromagnet including only nearest-neighbor magnetic interactions, within this first-order approximation the relative strength of magnon pair and higher-order magnon excitations is an intrinsic property of the spin system, depending only upon the excitations generated by $\mathbf{S}_i\cdot\mathbf{S}_j$.

The processes that generate multimagnon bands are related to those which generate zero-point fluctuation and hence, should scale similarly with S. Roughly, these should scale like $1-(M^{\dagger}/M_0)^2$, where $M^{\dagger}$ is the staggered magnetization and M_0 is the value it would have without quantum corrections. Using the results of Igarashi,[49] one finds that $1-(M^{\dagger}/M_0)^2$ is ~0.6 for $S=\frac{1}{2}$ and 0.4 for $S=1$. Thus, we would expect only a small decrease in the sideband strength from La_2CuO_4 to La_2NiO_4, of the order of a factor 2, compared with the actual value of a factor 50 or more. To examine the role of higher-order magnon excitations, Lorenzana

et al.[48] conducted exact diagonalization calculations on small model clusters. For spin-$\frac{1}{2}$ antiferromagnets, the calculated absorption spectra do show phonon plus four-magnon excitations, but with an integrated strength ~ 3 times less than the sharp-phonon plus two-magnon peak. Recall that, experimentally, the sideband strength in La_2CuO_4 is a factor of 5 or more, greater, not less, than the sharp-peak strength.

Canali and Girvin have theoretically examined the role of similar four-magnon excitations in Raman scattering.[50] They find for spin $\frac{1}{2}$ that the four-magnon contribution is small, only about 3% of the two-magnon contribution. They also find that the four-magnon contribution for $S=1$ is only ~ 3 times smaller than that for $S=\frac{1}{2}$, in accord with our scaling argument. Experimentally, four-magnon Raman scattering has been observed by Dietz *et al.*[51] in 3D antiferromagnets. The four-magnon scattering is roughly a factor of 30 weaker than the two-magnon scattering in NiO and weaker still in $KNiF_3$. Although the relative four-magnon contribution is expected to be larger in 2D materials, like La_2NiO_4, it is still apparently small as can be seen from the Raman spectrum in the lowest panel of Fig. 13.

Hence, we conclude that four-magnon excitations in a two-dimensional Heisenberg antiferromagnet including only two-body nearest-neighbor interactions cannot explain the strong sideband absorption observed in the spin-$\frac{1}{2}$ copper oxides. Lorenzana and co-workers[11,48] suggest that additional terms in the magnetic Hamiltonian similar to those proposed to explain the magnetic Raman scattering[52–54] might explain the strength of the broad absorption observed between ~ 0.4 and 1 eV. For example, exact diagonalization calculations of the magnetic Raman scattering find that including a 4-spin cyclical exchange interaction increases the relative strength of higher-order magnon excitations.[53] While presently no theory for such effects in absorption experiments exists, we emphasize that any such model would require an enhancement by two orders of magnitude of the relative strength of the higher-order multiexcitation processes relative to that of the lowest-order processes. An alternate explanation is that these bands have a different electronic origin than that of the sharp ~ 0.4-eV bimagnon peak.

One physically reasonable alternative, worthy of consideration, is that the broad 0.4- to 1-eV bands are phonon and magnon sidebands of a Cu crystal-field exciton. In the undoped lamellar copper oxides, the ground-state electronic configuration has one Cu $3d$ hole per Cu site. As summarized in the energy-level diagram of Fig. 1, the tetragonal crystal field splits the Cu $3d$ states into four levels with the Cu $3d_{x^2-y^2}$ being the lowest-energy Cu $3d$-hole state. Promotion of the $d_{x^2-y^2}$ hole to the higher-energy $d_{3z^2-r^2}$, d_{xy}, d_{xz}, or d_{yz} states yields the valence-conserving, crystal-field (d-d^*) excitons.[55] Because these excitations do not change the Cu-ion valence, the large 8–10-eV energy necessary to create Cu^{+1}-Cu^{+3} pairs, the Hubbard U, does not contribute to the exciton energy. Cluster calculations predict the Cu d-d^* exciton energies to be ~ 1–1.5 eV.[14–18]

In the undoped copper oxides, with just one hole per Cu site, all the crystal-field states have spin $\frac{1}{2}$ and hence, all the Cu^{+2} crystal-field excitons are spin allowed. In general, such spin-allowed crystal-field excitations are made weakly electric-dipole allowed by coupling to optical phonons. For example, this is the accepted explanation for the bands seen in NiO at 1 and 1.8 eV.[56,57] In La_2NiO_4, Perkins *et al.*[13] observe similar bands at ~ 1 and 1.6 eV. For both bands in La_2NiO_4, the absorption coefficient at the peak is $\sim 100\ cm^{-1}$ and the half width is ~ 0.3 eV. Similarly, in the isostructural materials K_2NiF_4 and Rb_2NiF_4, each with spin 1,[58] and in K_2CuF_4,[59] with spin $\frac{1}{2}$, phonon sidebands to spin-allowed crystal-field excitons are seen with comparable strength and width, albeit at energies above 1 eV. In fact, considering the strongest band observed in each material, the integrated absorption strength is the same to within a factor of about 2 for La_2NiO_4, K_2NiF_4, Rb_2NiF_4, and K_2CuF_4. Hence, by comparison with measured absorption bands in these isostructural materials, one expects phonon sidebands on the spin-allowed crystal-field excitons in the undoped copper oxides to yield absorption bands roughly 0.3-eV wide with a peak intensity of about $100\ cm^{-1}$, very similar to the ~ 0.6-eV band in La_2CuO_4.

We next examine which Cu d-d^* exciton could be associated with the 0.6-eV broadband. In a tetragonal (D_{4h}) approximation, La_2CuO_4 has seven dipole-allowed optical phonons.[39] These include four E_u modes with dipole moments in the Cu-O plane and three A_{2u} modes polarized perpendicular to the Cu-O plane. Accordingly, phonon sidebands on the $d_{x^2-y^2} \rightarrow d_{3z^2-r^2}$ and $d_{x^2-y^2} \rightarrow d_{xy}$ crystal-field excitons should occur only for the optical electric field polarized parallel to the Cu-O plane whereas phonon sidebands on the $d_{x^2-y^2} \rightarrow d_{xz}$ and $d_{x^2-y^2} \rightarrow d_{yz}$ excitons should occur for the electric field polarized either parallel or perpendicular to the Cu-O plane. As evident in Fig. 2(b), the absorption bands occur only with the incident electric field polarized parallel to the Cu-O plane. Hence, the 0.6-eV band could be a phonon sideband only on either the $d_{x^2-y^2} \rightarrow d_{3z^2-r^2}$ or $d_{x^2-y^2} \rightarrow d_{xy}$ crystal-field excitons.

Recent electroreflectance experiments by Falck *et al.*[5] on La_2CuO_4 and large energy shift Raman-scattering experiments by Liu *et al.*[6] and Salamon *et al.*[7] on eight different undoped copper oxides find A_{2g} ($d_{x^2-y^2} \rightarrow d_{xy}$) symmetry excitations near 1.5 eV. Recall that we observe an additional absorption band near 1.5 eV in both La_2CuO_4 and $Sr_2CuO_2Cl_2$ as shown in Fig. 4. If these ~ 1.5-eV excitations are indeed associated with the $d_{x^2-y^2} \rightarrow d_{xy}$ exciton, then the only Cu d-d^* exciton, consistent with our data, that could exist at ~ 0.5 eV is the Cu $d_{x^2-y^2} \rightarrow d_{3z^2-r^2}$ exciton. We note that cluster calculations generally predict the $d_{x^2-y^2} \rightarrow d_{3z^2-r^2}$ exciton to be the lowest-energy d-d^* exciton; however, the predicted energies range from 1–1.5 eV.[14–18] Interestingly, the Raman-scattering experiments that identified the $d_{x^2-y^2} \rightarrow d_{xy}$ exciton at ~ 1.5 eV, find no $d_{x^2-y^2} \rightarrow d_{3z^2-r^2}$ exciton between 1 and 2 eV.[6,7]

For the $d_{x^2-y^2} \rightarrow d_{3z^2-r^2}$ exciton, magnon as well as phonon sidebands are possible. Electric-dipole-allowed exciton-magnon absorption was first seen in MnF_2 by Greene *et al.*[60] in 1965. Its subsequent observation in ten additional antiferromagnetic insulators by 1968 (Ref. 61) established joint exciton-magnon excitation as a fundamental intrinsic excitation of antiferromagnetic insulators. The commonly accepted microscopic explanation, based on off-diagonal exchange, was put forth by Tanabe, Moriya, and Sugano[62] in 1965 and predicts weakly allowed electric-dipole absorption.[63–67]

The magnon sideband energies can be estimated using a simple Ising model. Consider two nearest-neighbor Cu sites, *A* and *B*, on a 2D square lattice. In accord with the Tanabe model, the exciton-magnon state corresponds to creating an exciton plus a spin flip at site *A* along with a spin flip at site *B*. Thus, two spins have the opposite orientation of that favored by the antiferromagnetic exchange. For $S=\frac{1}{2}$, each resulting ferromagnetically aligned pair of nearest-neighbor spins adds $\frac{1}{2}J$ to the energy, where J is the ground-state $d_{x^2-y^2}$-$d_{x^2-y^2}$ nearest-neighbor Heisenberg exchange. For spins coupled to the spin on the exciton site, the exchange coupling is different, J'. Hence, the first magnon sideband should be peaked at $\sim\frac{3}{2}(J+J')$ above the exciton energy. For Cu d-d^* excitons we expect a substantially reduced J'; from overlap considerations alone, $J'=J/3$ (Ref. 68) for the $d_{3z^2-r^2}$ exciton and $J'=0$ for the d_{xy}, d_{xz}, and d_{yz} excitons. Considering the $d_{3z^2-r^2}$ exciton and taking $J=0.13$ eV, this simple model predicts the first magnon sideband should occur $2J\sim0.26$ eV above the exciton energy. Hence, an exciton energy of $\sim$0.5 eV as suggested above, yields the first magnon sideband peak at $\sim$0.75 eV, close to the observed value of the second broadband maximum in La_2CuO_4 as evident in Fig. 13.

Although the integrated strength of the $\sim$0.75-eV band is several orders of magnitude stronger than that for previously observed exciton-magnon sidebands such as in $RbMnF_3$ (Ref. 69) or MnF_2,[60] it is consistent with expectations for joint exciton-magnon absorption. Examination of the coupling constants,[63–67] as discussed in Perkins *et al.*,[4] indicates that the integrated strength of the sidebands should scale very roughly as the square of the exchange energy. In the manganese fluorides the integrated absorption strength is of order 10^3 cm^{-2} while the ratio of zone-boundary magnon energies squared between La_2CuO_4 and the fluorides is $\sim10^3$. This suggests an integrated strength for magnon sideband absorption in La_2CuO_4 of order 10^6 cm^{-2} in agreement with the observed strength that is indeed $\sim10^6$ cm^{-2}. There is great uncertainty in this comparison because of the different crystal structures, in the states involved in the exciton for the two materials, and in the width of the sidebands in the Cu oxides. Nonetheless, the overall order of magnitude is reasonable.

To our knowledge, electric-dipole-allowed magnon sidebands on a spin-allowed crystal-field exciton have not been previously observed. This can be easily understood in terms of the preceding discussion. Consider K_2NiF_4 with $J\sim77$ cm^{-1}.[70] Using a $(JS)^2$ scaling for the integrated oscillator strength, the expected absorption would be 100 times weaker than in La_2CuO_4 and, hence, much smaller than the phonon sideband absorption. In addition, the energy shift of the magnon sideband, which scales with J, would be $\approx$0.02 eV. Thus, in K_2NiF_4, magnon sidebands on the spin-allowed crystal-field excitations are likely unobservable due to masking by the much stronger and broader phonon sidebands. However, in materials with a large exchange energy, such as La_2CuO_4, the magnon sidebands should be both strong enough and have large enough energy shifts to be observable along with the phonon sidebands. For spin-forbidden excitons, as in Rb_2MnF_4, the phonon sidebands are strongly suppressed, thereby permitting observation of the magnon sidebands.[66]

Next we consider the low, $\sim$0.5 eV, energy for the Cu $d_{x^2-y^2}\rightarrow d_{3z^2-r^2}$ exciton necessary to explain the broad absorption. Several other experimental quantities are relevant to this discussion; among them are the g value and Van Vleck susceptibility. In general, the relative energies of the d-d^* excitons affect the anisotropies in the g value, and thereby the spin susceptibility and anisotropic exchange, as well as the Van Vleck susceptibility. The observed anisotropies[71–73] are consistent with $d_{x^2-y^2}\rightarrow d_{xy}$ and $d_{x^2-y^2}\rightarrow d_{xz}$, d_{yz} energies of $\sim$1.5 eV or greater. However, since the $d_{x^2-y^2}$ and $d_{3z^2-r^2}$ states are not coupled by L, the $d_{x^2-y^2}\rightarrow d_{3z^2-r^2}$ exciton energy does not affect the anisotropic susceptibilities.[74] Hence, of the four d-d^* excitons, only the $d_{x^2-y^2}\rightarrow d_{3z^2-r^2}$ exciton could be at $\sim$0.5 eV.

Polarized x-ray-absorption spectroscopy (XAS) can probe excitations similar to the Cu d-d^* excitons. In oxygen *K*-line absorption in the doped copper oxides, an $O1s$ electron is excited to fill an $O2p$ valence hole. For such an excitation, the final state of the hole on the adjacent Cu may be either the Cu $d_{x^2-y^2}$ or $d_{3z^2-r^2}$ orbital. Thus, if these two states differed in energy by 1–1.5 eV as predicted by cluster calculations, two lines would be observed. Experiments by Bianconi and co-workers[75,76] show a single line, but one that is broader than the experimental resolution. Accordingly, the authors put an upper limit on the $d_{x^2-y^2}\rightarrow d_{3z^2-r^2}$ splitting of $\sim$0.5 eV. This interpretation is supported by calculations that show that a small $d_{x^2-y^2}\rightarrow d_{3z^2-r^2}$ splitting is required to account for the doped hole's Cu $d_{3z^2-r^2}$ character as measured by XAS.[77–79] However, we note that both the experiments and this interpretation are disputed in the literature.[80,81]

If the lowest-energy broadband at $\sim$0.6 eV arises from phonon sidebands on the Cu $d_{x^2-y^2}\rightarrow d_{3z^2-r^2}$ crystal-field exciton, then, as evident in Fig. 13, the $d_{x^2-y^2}\rightarrow d_{3z^2-r^2}$ exciton energy must be similar in La_2CuO_4, $Sr_2CuO_2Cl_2$, and Nd_2CuO_4. This might at first seem surprising given the differing out-of-plane structures in these materials. Recall that, while in La_2CuO_4 the Cu ions are octahedrally coordinated with apical oxygen ions, $Sr_2CuO_2Cl_2$ has apical Cl ions and Nd_2CuO_4 is square planar with no apical ions. Therefore, the exciton interpretation requires that the strong Cu-O in-plane bonding dominates the exciton energies.

V. SUMMARY

The sharp peak near 0.4 eV and the broadbands extending up to 1 eV are clearly intrinsic, weakly electric-dipole allowed, excitations of the undoped CuO_2 layer. The line shape of the sharp peak and that of a related peak in La_2NiO_4 are quantitatively described by the theory of Lorenzana and Sawatzky[11,12] for one-phonon–two-magnon absorption. However, both the absence of the broadbands in La_2NiO_4 compared to their dominance in La_2CuO_4 and the large relative intensity of the broadbands in La_2CuO_4 are not only inconsistent with the existing models, but further suggest that these bands may arise from processes other than phonon-multimagnon excitations. In our view, for phonon-assisted magnetic excitations to explain the observed differences between $S=1$ La_2NiO_4 and $S=\frac{1}{2}$ La_2CuO_4 would require additional unknown interactions which somehow enhance the broadband absorption in the copper oxides by two or more

orders of magnitude. We argue that phonon and magnon sidebands of a Cu d-d^* exciton are a plausible explanation. Such an exciton-based origin accounts for the structure, strength, and polarization dependence of the 0.4–1-eV bands.

The most controversial implication of d-d^* exciton picture is the low, ~0.4 to 0.5 eV, energy required for the Cu $d_{x^2-y^2} \rightarrow d_{3z^2-r^2}$ exciton. This is significantly lower than the 1–1.5 eV predicted by cluster calculations.[14–18] Raman-scattering experiments, which should be sensitive to the $d_{x^2-y^2} \rightarrow d_{3z^2-r^2}$ exciton and do observe the $d_{x^2-y^2} \rightarrow d_{xy}$ exciton at ~1.5 eV, find no evidence for the $d_{x^2-y^2} \rightarrow d_{3z^2-r^2}$ exciton between 1 and 2 eV.[6,7] However, the $d_{x^2-y^2} \rightarrow d_{3z^2-r^2}$ exciton has the same B_{1g} symmetry as the two-magnon Raman scattering, which, in the copper oxides, is peaked at ~0.4 eV with a high-energy tail extending to almost 1 eV. Hence, it is possible that a $d_{x^2-y^2} \rightarrow d_{3z^2-r^2}$ exciton at ~0.4 to 0.5 eV may either contribute to, or be masked by, the magnetic Raman scattering.

Clearly, independent experiments to determine the Cu $d_{x^2-y^2} \rightarrow d_{3z^2-r^2}$ exciton energy would be valuable and, in particular, would present a critical test of the exciton sideband model. For example, using low-energy electron-energy-loss spectroscopy, dipole-forbidden d-d^* excitations have recently been measured in NiO and CoO via electron exchange scattering.[82–84] Alternatively, electroreflectance measurements in a suitable geometry could examine the $d_{x^2-y^2} \rightarrow d_{3z^2-r^2}$ exciton. In addition, both experiments and calculations studying the possible role of higher-order magnetic interactions would be valuable. Lastly, dedicated experiments are needed to examine the effects of doping upon the intrinsic absorption spectra presented in this work.

ACKNOWLEDGMENTS

The authors thank J. Lorenzana and G. Sawatzky for informative discussions on their work prior to publication. We thank A. Cassanho, J. P. Falck, M. Greven, and H. Jenssen for some of the crystals used in these measurements. We also thank C. Castellani, S. Girvin, M. Klein, P. Littlewood, R. Liu, and A. McMahon for helpful discussions. J.D.P. acknowledges support from the National Renewable Energy Laboratory while preparing the manuscript. This work was supported in part by the MRSEC Program of the National Science Foundation under award No. DMR 94-00334 and in part by the National Science Foundation under award No. DMR 94-1174.

*Present address: National Renewable Energy Laboratory, Golden, CO 80401.

†Present address: Department of Physics, University of Florida, Gainesville, FL 32611.

[1] S. Uchida, T. Ido, H. Takagi, T. Arima, Y. Tokura, and S. Tajima, Phys. Rev. B **43**, 7942 (1991).

[2] D. B. Tanner and T. Timusk, in *Physical Properties of High-Temperature Superconductors III*, edited by D. Ginsberg (World Scientific, Singapore, 1992).

[3] G. A. Thomas, in *High Temperature Superconductivity*, edited by D. P. Tunstall and W. Barford (Hilger, Bristol, 1991), p. 169.

[4] J. D. Perkins, J. M. Graybeal, M. A. Kastner, R. J. Birgeneau, J. P. Falck, and M. Greven, Phys. Rev. Lett. **71**, 1621 (1993).

[5] J. P. Falck, J. D. Perkins, A. Levy, M. A. Kastner, J. M. Graybeal, and R. J. Birgeneau, Phys. Rev. B **49**, 6246 (1994).

[6] R. Liu, D. Salamon, M. V. Klein, S. L. Cooper, W. C. Lee, S.-W. Cheong, and D. M. Ginsberg, Phys. Rev. Lett. **71**, 3709 (1993).

[7] D. Salamon, R. Liu, M. V. Klein, M. A. Karlow, S. L. Cooper, S.-W. Cheong, W. C. Lee, and D. M. Ginsberg, Phys. Rev. B **51**, 6617 (1995).

[8] G. A. Thomas, D. H. Rapkine, S. L. Cooper, S.-W. Cheong, A. S. Cooper, L. F. Schneemeyer, and J. V. Waszczak, Phys. Rev. B **45**, 2474 (1992).

[9] J. P. Falck, A. Levy, M. A. Kastner, and R. J. Birgeneau, Phys. Rev. B **48**, 4043 (1993).

[10] M. Grüninger, J. Münzel, A. Gaymann, A. Zibold, H. P. Geserich, and T. Kopp, Europhys. Lett. **35**, 55 (1996).

[11] J. Lorenzana and G. A. Sawatzky, Phys. Rev. B **52**, 9576 (1995).

[12] J. Lorenzana and G. A. Sawatzky, Phys. Rev. Lett. **74**, 1867 (1995).

[13] J. D. Perkins, D. S. Kleinberg, M. A. Kastner, R. J. Birgeneau, Y. Endoh, K. Yamada, and S. Hosoya, Phys. Rev. B **52**, R9863 (1995).

[14] J. B. Grant and A. K. McMahon, Phys. Rev. Lett. **66**, 488 (1991).

[15] J. B. Grant and A. K. McMahan, Phys. Rev. B **46**, 8440 (1992).

[16] J. Ghijsen, L. H. Tjeng, J. van Elp, H. Eskes, J. Westerink, G. A. Sawatzky, and M. T. Czyzyk, Phys. Rev. B **38**, 11 322 (1988).

[17] H. Eskes, L. H. Tjeng, and G. A. Sawatzky, Phys. Rev. B **41**, 288 (1990).

[18] R. L. Martin and P. J. Hay, J. Chem. Phys. **98**, 8680 (1993).

[19] K. B. Lyons, P. E. Sulewski, P. A. Fleury, H. L. Carter, A. S. Cooper, G. P. Espinosa, Z. Fisk, and S.-W. Cheong, Phys. Rev. B **39**, 9693 (1989).

[20] Y. Tokura, S. Koshihara, T. Arima, H. Takagi, S. Ishibashi, T. Ido, and S. Uchida, Phys. Rev. B **41**, 11 657 (1990).

[21] S. L. Cooper, G. A. Thomas, A. J. Millis, P. E. Sulewski, J. Orenstein, D. H. Rapkine, S.-W. Cheong, and P. L. Trevor, Phys. Rev. B **42**, 10 785 (1990).

[22] S. Sugai, M. Sato, T. Kobayashi, J. Akimitsu, T. Ito, H. Takagi, S. Uchida, S. Hosoya, T. Kajitani, and T. Fukuda, Phys. Rev. B **42**, 1045 (1990).

[23] K. Nakajima, K. Yamada, S. Hosoya, T. Omata, and Y. Endoh, J. Phys. Soc. Jpn. **62**, 4438 (1993).

[24] M. Greven, R. J. Birgeneau, Y. Endoh, M. A. Kastner, M. Matsuda, and G. Shirane, Z. Phys. B **96**, 465 (1995).

[25] P. J. Picone, H. P. Jenssen, and D. R. Gabbe, J. Cryst. Growth **85**, 576 (1987).

[26] Y. Hidaka, T. Enomoto, M. Suzuki, M. Oda, and T. Murakami, J. Cryst. Growth **85**, 581 (1987).

[27] I. Tanaka and H. Kojima, Nature (London) **337**, 21 (1989).

[28] N. W. Preyer, R. J. Birgeneau, C. Y. Chen, D. R. Gabbe, H. P. Jenssen, M. A. Kastner, P. J. Picone, and T. Thio, Phys. Rev. B **39**, 11 563 (1989).

[29] C. Y. Chen, R. J. Birgeneau, M. A. Kastner, N. W. Preyer, and T. Thio, Phys. Rev. B **43**, 392 (1991).

[30] J. P. Falck, A. Levy, M. A. Kastner, and R. J. Birgeneau, Phys. Rev. Lett. **69**, 1109 (1992).

[31] L. L. Miller, X. L. Wang, S. X. Wang, C. Stassis, D. C. Johnston, J. Faber, Jr., and C.-K. Loong, Phys. Rev. B **41**, 1921 (1990).

[32] D. Vaknin, S. K. Sinha, C. Stassis, L. L. Miller, and D. C.

Johnston, Phys. Rev. B **41**, 1926 (1990).
[33] S. Jandl, P. Dufour, T. Strach, T. Ruf, M. Cardona, V. Nekvasil, C. Chen, and B. M. Wanklyn, Phys. Rev. B **52**, 15 558 (1995).
[34] M. L. Jones, D. W. Shortt, B. W. Sterling, A. L. Schawlow, and R. M. Macfarlane, Phys. Rev. B **46**, 611 (1992).
[35] T. Thio, R. J. Birgeneau, A. Cassanho, and M. A. Kastner, Phys. Rev. B **42**, 10 800 (1990).
[36] Y. H. Kim, S.-W. Cheong, and Z. Fisk, Phys. Rev. Lett. **67**, 2227 (1991).
[37] Momentum in units for the 2D CuO_2 layer with the Cu-Cu bond distance=1.
[38] L. Pintschovius, N. Pyka, W. Reichardt, A. Y. Rumiantsev, N. L. Mitrofanov, A. S. Ivanov, G. Collin, and P. Bourges, Physica C **185**, 156 (1991).
[39] L. Pintschovius, J. M. Bassat, P. Odier, F. Gervais, G. Chevrier, W. Reichardt, and F. Gompf, Phys. Rev. B **40**, 2229 (1989).
[40] K. B. Lyons, P. A. Fleury, J. P. Remeika, A. S. Cooper, and T. J. Negran, Phys. Rev. B **37**, 2353 (1988).
[41] R. R. P. Singh, P. A. Fleury, K. B. Lyons, and P. E. Sulewski, Phys. Rev. Lett. **62**, 2736 (1989).
[42] S. M. Hayden, G. Aeppli, R. Osborn, A. D. Taylor, T. G. Perring, S.-W. Cheong, and Z. Fisk, Phys. Rev. Lett. **67**, 3622 (1991).
[43] R. E. Dietz, G. I. Parisot, and A. E. Meixner, Phys. Rev. B **4**, 2302 (1971).
[44] A. Tsuchida, J. Phys. Soc. Jpn. **21**, 2497 (1966).
[45] S. R. Chinn, H. J. Zeiger, and J. R. O'Connor, Phys. Rev. B **3**, 1709 (1971).
[46] S. Tajima, T. Ido, S. Ishibashi, T. Itoh, H. Eisaki, Y. Mizuo, T. Arima, H. Takagi, and S. Uchida, Phys. Rev. B **43**, 10 496 (1991).
[47] We use ''multimagnon'' to refer to excitations involving more than two magnons.
[48] J. Lorenzana, R. Eder, M. Meinders, and G. A. Sawatzky, J. Supercond. **8**, 567 (1995).
[49] J. Igarashi, Phys. Rev. B **46**, 10 763 (1992).
[50] C. M. Canali and S. M. Girvin, Phys. Rev. B **45**, 7127 (1992).
[51] R. E. Dietz, W. F. Brinkman, A. E. Meixner, and H. J. Guggenheim, Phys. Rev. Lett. **27**, 814 (1971).
[52] S. Sugai, Solid State Commun. **75**, 795 (1990).
[53] Y. Honda, Y. Kuramoto, and T. Watanabe, Phys. Rev. B **47**, 11 329 (1993).
[54] P. E. Sulewski, P. A. Fleury, K. B. Lyons, and S.-W. Cheong, Phys. Rev. Lett. **67**, 3864 (1991).
[55] Strictly speaking, we should call these ligand-field excitons because of the large covalency of the Cu-O bond; we use the term crystal field for convenience.
[56] C. J. Ballhausen, *Introduction To Ligand Field Theory* (McGraw-Hill, New York, 1962), p. 261.
[57] R. Newman and R. M. Chrenko, Phys. Rev. **114**, 1507 (1959).
[58] K. Iio and K. Nagata, J. Phys. Soc. Jpn. **41**, 1550 (1976).
[59] R. Laiho, Phys. Status Solidi B **69**, 579 (1975).
[60] R. L. Greene, D. D. Sell, W. M. Yen, A. L. Schawlow, and R. M. White, Phys. Rev. Lett. **15**, 656 (1965).
[61] D. D. Sell, J. Appl. Phys. **39**, 1030 (1968).
[62] Y. Tanabe, T. Moriya, and S. Sugano, Phys. Rev. Lett. **15**, 1023 (1965).
[63] K. Gondaira and Y. Tanabe, J. Phys. Soc. Jpn. **21**, 1527 (1966).
[64] Y. Tanabe and K. Gondaira, in *Optical Properties of Ions in Crystals*, edited by H. H. Crosswhite and H. W. Moos (Wiley, New York, 1966).
[65] Y. Tanabe and K. Aoyagi, in *Excitons*, edited by E. I. Rashba and M. D. Sturge (North-Holland, Amsterdam, 1982).
[66] J. B. Parkinson, J. Phys. C **2**, 2012 (1969).
[67] J. B. Parkinson and R. Loudon, J. Phys. C **1**, 1568 (1968).
[68] In Ref. 5, an incorrect value $J'=J/6$ was used.
[69] R. S. Meltzer, M. Y. Chen, D. S. McClure, and M. Lowe-Pariseau, Phys. Rev. Lett. **21**, 913 (1968).
[70] P. A. Fleury and H. J. Guggenheim, Phys. Rev. Lett. **24**, 1346 (1970).
[71] T. Thio, T. R. Thurston, N. W. Preyer, P. J. Picone, M. A. Kastner, H. P. Jenssen, D. R. Gabbe, C. Y. Chen, R. J. Birgeneau, and A. Aharony, Phys. Rev. B **38**, 905 (1988).
[72] T. Thio, Ph.D. thesis, Massachusetts Institute of Technology, 1988.
[73] V. Likodimos, N. Guskos, G. Palios, A. Koufoudakis, J. Typek, B. Bojanowski, and M. Wabia, Phys. Rev. B **52**, 7682 (1995).
[74] G. Sawatzky (private communication).
[75] A. Bianconi, C. Li, S. D. Longa, and M. Pompa, Phys. Rev. B **45**, 4989 (1992).
[76] C. Li, M. Pompa, S. D. Longa, and A. Bianconi, Physica C **178**, 421 (1991).
[77] M. Grilli, C. Castellani, and C. Di Castro, Phys. Rev. B **42**, 6233 (1990).
[78] L. F. Feiner, M. Grilli, and C. Di Castro, Phys. Rev. B **45**, 10 647 (1992).
[79] F. Bucci, C. Castellani, C. Di Castro, and M. Grilli, Phys. Rev. B **52**, 6880 (1995).
[80] C. T. Chen, L. H. Tjeng, J. Kwo, H. L. Kao, P. Rudolf, F. Sette, and R. M. Fleming, Phys. Rev. Lett. **68**, 2543 (1992).
[81] E. Pellegrin, N. Nücker, J. Fink, S. L. Molodtsov, A. Gutiérrez, E. Navas, O. Strebel, Z. Hu, M. Domke, G. Kaindl, S. Uchida, Y. Nakamura, J. Markl, M. Klauda, G. Saemann-Ischenko, A. Krol, J. L. Peng, Z. Y. Li, and R. L. Greene, Phys. Rev. B **47**, 3354 (1993).
[82] A. Gorschlüter and H. Merz, Phys. Rev. B **49**, 17 293 (1994).
[83] B. Fromme, M. Schmitt, E. Kisker, A. Gorschlüter, and H. Merz, Phys. Rev. B **50**, 1874 (1994).
[84] B. Fromme, C. Koch, R. Deussen, and E. Kisker, Phys. Rev. Lett. **75**, 693 (1995).